A Distributed Adaptive Sampling Soluting using Autonomous Underwater Vehicles

Baozhi Chen, Parul Pandey, and Dario Pompili
Department of Electrical and Computer Engineering
Rutgers University, New Brunswick, NJ
{baozhi_chen, parul_pandey, pompili}@cac.rutgers.edu

ABSTRACT

To achieve efficient and cost-effective sensing coverage of the vast under-sampled 3D aquatic volume, intelligent adaptive sampling strategies involving a team of Autonomous Underwater Vehicles (AUVs) endowed with underwater wireless communication capabilities become essential. Given a 3D field of interest to sample, the AUVs should coordinate to take measurements using minimal resources (time or energy) in order to reconstruct the field at an onshore station with admissible error. A novel distributed adaptive sampling solution that can minimize the sampling cost (in terms of time or energy expenditure) is proposed along with underwater acoustic communication protocols that facilitate the coordination of the vehicles. The proposed solution operates in two distinct phases in which it employs random compressive sensing (Phase I) and adaptive sampling (Phase II). Phase I captures the spatial distribution of the field of interest while Phase II tracks the temporal variation of the same. A distributed framework for multi-vehicle adaptive sampling that facilitates the movement of data between AUVs and enables compute intensive adaptive sampling algorithms is proposed. Simulation results on real data traces show that the proposed adaptive sampling solution significantly outperforms existing solutions in terms of reconstruction accuracy and energy expenditure.

Categories and Subject Descriptors

C.2.1 [**Computer Systems Organization**]: Network Architecture and Design—*Distributed networks, Network communications, Wireless communication*

General Terms

Algorithms, Performance, Design

1. INTRODUCTION

Ocean weather forecast relies on the state of the fluid sampled (such as temperature) at a given time and uses the equations of fluid dynamics and thermodynamics to predict the future state of the fluid [1]. It is known that a small uncertainty in the initial and boundary conditions (such as ocean surface temperature) may lead to large deviation in real-time ocean forecasting [2]. To minimize such deviation in ocean forecasting, accurate reconstruction of the ocean scalar field is therefore necessary. Existing observation solutions using satellites, lack depth information; whereas using static observation networks (e.g., networked buoys) may not be optimal as sampling regions of different dynamics requires the ability to change the spatial distribution of sensors. Consequently, there is a need for adaptive sampling solutions as the sensors should be deployed and moved dynamically for optimal sampling performance. This is achieved using a team of Autonomous Underwater Vehicles (AUVs), which can coordinate to sample the phenomenon.

To be able to perform adaptive sampling, the AUVs need to adjust on the fly their trajectory, inter-vehicle distance, or formation based on real-time field measurements. In [3], we proposed team formation and steering algorithms for a team of AUVs. In this work the AUVs steer through the 3D region of interest while forming a team in a specific formation and take application-dependent measurements such as temperature and salinity. The sampling technique employed in this work was not adaptive and took samples at pre-defined locations. Several adaptive sampling solutions for measurement of ocean physical and chemical processes using AUVs have been proposed such as [4, 5]. These solutions focus on sampling a given region in such a way as to maximize a certain objective function, e.g., the gradient of the process, or the path that maximizes the line integral of uncertainty of field along that path. The goal of adaptive sampling is to improve the accuracy of estimates of field of interest by utilizing the available resources at hand in an optimal manner. As pointed out in [4] the estimates can be 1) the nowcast fields, which determine the data needed now to best improve the current estimates; 2) the forecast fields, which determine the data needed to improve the prediction of field; 3) the past fields, which determine the data that minimizes the error in the initial conditions.

Recently, Random Compressive Sensing (RCS) and Deterministic Compressive Sensing (DCS) techniques have been proposed, which offer a novel way to capture and reconstruct a signal using minimal number of samples [6]. These techniques offer a promising solution for reconstructing a field of interest efficiently from a small number of measurements and therefore has the potential to be used in sampling solutions. The major drawback of these techniques is that they do not take into account the real-time characteristics of the field to estimate the locations from where samples should be taken, which makes them unsuitable to implement adaptive sampling strategies. For example, to accurately reconstruct a temperature field, regions with relatively constant (i.e., low varying) temperature values should be sampled at a lower rate (in space) than regions with large variations in temperature. The CS tech-

niques are not able to exploit the distinction between the rate of spatial sampling based on features of regions in the field of interest.

For this reason, in this work, we propose a novel adaptive sampling solution for AUVs to reconstruct a scalar ocean phenomenon (e.g., temperature). We first obtain a preliminary *spatial* estimate of the field (Phase I) and then adaptively sample locations in order to track the *temporal variations* in the field (Phase II) while minimizing the energy expenditure for sampling. For Phase I we estimate the field using RCS technique to capture the spatial variations in the field, and for Phase II we use an optimization algorithm where the objective function is to minimize the energy consumption while keeping the error below a pre-specified limit. In both Phase I and Phase II we aggregate the data from different AUVs in a team for global reconstruction of the field. We propose a distributed computing framework to support data exchange between AUVs and compute intensive tasks such as reconstruction of field and solving the optimization algorithm. Our contributions in this paper are as follows:

- We not only capture the spatial distribution of a scalar field of interest but also track its temporal variations by adaptively sampling (in space and time) using a team of AUVs. We select the sampling locations by minimizing a cost function that represents the energy expenditure.

- We propose a distributed framework to enable compute intensive adaptive sampling algorithms, and exchange of data among AUVs in a team for global reconstruction of the field from collected samples.

The remainder of this paper is organized as follows: in Sect. 2, we review related work for adaptive sampling in underwater sensor networks, in Sect. 3, we describe our proposed two-phase adaptive sampling solution as well as our distributive computing framework; in Sect. 4, we evaluate the performance of our proposed approach; finally, in Sect. 5, we draw the conclusions and provide a brief note on future work.

2. RELATED WORK

Adaptive sampling solutions follow two approaches namely, data driven or model driven. In [7] a data-driven adaptive sampling algorithm is presented. The region is sampled using a team of AUVs but no particular formation is enforced by the team. The algorithm selects samples such that a desired accuracy in reconstruction is maintained and at the same time cooperation algorithm ensures that each vehicle is able to communicate with its closest neighbor while maximizing the local distance among AUVs. Other rules such as taking samples in area where present sampling density is lower and avoiding areas where measurements had been already taken are also imposed while taking new samples. The reconstruction is based on properties of Radial Basis Functions (RBFs).

In [8] also a data-driven approach is presented. The approach presented is similar to [7] and differs only in the way AUVs communicate with each other. The approach presents a graph-based structure for communication between AUV. Every time a new sampling measurement has to be taken by a node it communicates with its predecessor and successor node, which leads to heavy communication burden on the node unlike [7] where AUVs communicate only with their nearest neighbor. This technique is also very sensitive to loss of communication among the vehicles.

We present a data-driven approach where a team of AUVs maintains a formation and selects samples by minimizing energy consumed while keeping the error bounded. The communication between AUVs is minimal and they need to exchange data only after scanning a region unlike the above mentioned algorithm where AUVs communicate every time a new location has to be selected.

In [9], the authors present an adaptive sampling algorithm for multiple autonomous underwater vehicles using model approach. Given the position of an AUV, the next sampling location is modeled using a kinematic model and the solution to it is given using Extended Kalman Filter. The model assumes that field variable, e.g., temperature varies with linearly with location. A divergence function is calculated that measures the dissimilarity between present sampling location and next sampling location. The algorithm selects the new sampling location such as to minimizes the divergence function.

In [4] the authors present a path planning algorithm using adaptive sampling techniques. Here, the goal is to find the vehicle path that maximizes the line integral of the uncertainty of field estimates along this path. The uncertainty region which is the input to the objective function could be a probability distribution field or physical features of dynamical interest e.g, eddies, upwelling etc. Several constraints are mentioned to achieve this objective, e.g, motion constraint on vehicles, anticurling constraint, vicinity constraint constraint for multiple vehicle case to avoid collisions, constraints to avoid obstacle collisions, and constraints to maintain radio communication between shore station and AUVs. Our solution on the other hand does not require any uncertainty region as an input to the objective function unlike the above approach.

The number of research works that apply Compressive Sensing (CS) techniques to sample a region is relatively small for robotics, not to mention underwater robotics. The CS techniques allow the reconstruction of a phenomenon with only a subset of samples and hence save time and energy. In [10], trajectory planning algorithms based on the standard compressive sensing paradigm are presented for robots following different mobility patterns - including Random Walk, Random Traveling Salesman Problem, and Randomized Boustrophedon - to take samples. A cost function is proposed to evaluate the energy spent in taking measurement at a point and measurements are taken at positions where the expected cost function is close to the available energy. Using the random measurements from these trajectories, the entire field of interest is reconstructed using compressive sensing.

A scenario where a randomly subset of underwater sensor nodes is chosen to send data frames that contain sampled data to the fusion center is presented in [11]. Due to the packet loss resulted from random access collisions, only a subset of data packets are received by the fusion center. However, using compressive sensing, the entire field of interest can be recovered without retransmissions, overcoming the challenge of limited energy and bandwidth.

Our approach differs from these compressive sensing approaches as these do not take into account the underlying data while sampling the field. We use compressive sensing techniques to get a preliminary estimate of the image and then adaptively sample the region unlike the above approach which only rely on the collection of samples by compressive sensing.

3. PROPOSED SOLUTION

In this section, we present the details of our proposed solution. To sample a region of interest, AUVs move across a field by following a certain trajectory and take samples as they move. For example, one conventional method to do this is to steer the AUVs in a lawn-mower style and take samples at equidistant positions: such method is, however, inefficient as the AUVs need to scan through the whole region without considering the characteristics of the field. Conversely, efficient solutions can be developed that take samples
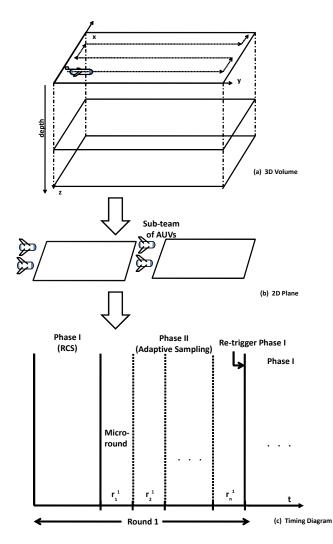
Figure 1: Block (a) shows ocean as a 3D volume, (b) The 3D volume is divided into multiple 2D planes. (c) Timing Diagram of Phases I and II, which occur while sampling a 2D plane.

at a smaller number of locations so to reduce the cost (such as energy or error) incurred to reconstruct the field.

We present our solution that minimizes a cost (in terms of energy expenditure or reconstruction error depending on the application requirements) to sample adaptively (in space and in time) a region of interest and to track the temporal variations in the field. We could use either of the two cost function based on the high level requirement of oceanographer but in this paper we for the sake of clarity we use energy expenditure as the cost function. We build on our previous work on adaptive sampling in [12]. The 3D volume of ocean (as shown in Fig. 1) can be divided into multiple 2D horizontal planes. For propeller based underwater vehicles this is the most energy efficient way of dividing the 3D volume but our framework can be extended to gliders too that follow a vertical plane. There are two significant challenges with this approach, i) how to optimally partition a team of AUVs in to sub-teams that can adaptively scan the individual 2D planes, and ii) how can a sub-team of AUVs adaptively sample (in both space and time) the 2D horizontal plane with the objective of minimizing energy expenditure while satisfying a pre-specified reconstruction accuracy. The first problem is task-allocation problem while the second is an adaptive sampling

problem. In this paper, we focus on the adaptive sampling problem.

Our adaptive sampling solution consists of many *rounds*. Each round of our solution operates in two phases, Phase I captures the spatial distribution of a manifestation (say salinity, or temperature) in the field of interest while Phase II tracks the temporal variations of the manifestation. Both the phases together form a *round*, which is repeated over time. The two phases are shown in the timing diagram in Fig. 1(c). In Phase I, the field is scanned *randomly* to obtain a preliminary estimate of the spatial distribution of the manifestation in the field (through compressive sensing); and in Phase II, the field is scanned *adaptively,* in multiple *micro-rounds,* to capture the temporal variations. Micro-rounds in Phase II are *repeated* until the reconstructed field in a micro-round varies significantly from the field's initial estimate in Phase I (by a pre-specified threshold). At this point, one round is deemed completed and the next round begins with a re-triggering of Phase I followed by Phase II. In this section, we also discuss a strategy for optimization of communication parameters, e.g., transmit power, number of samples, and the best neighbor vehicle, in order to enable reliable inter-AUV communication.

3.1 Multi-Vehicle Adaptive Sampling

We now discuss both phases of our solution in detail. First, we explain how the preliminary estimate of the field is obtained and then we describe how our adaptive sampling solution tracks the temporal variations.

Phase I: In this phase, our solution gives us preliminary estimate of the field by using RCS. RCS is done to get the spatial structure of the field under consideration. Later we present traveling salesman problem which determines the trajectory of vehicles to scan the region in a time efficient manner.

Random Compressive Sensing: In RCS, a sparse signal $\mathbf{x} \in \mathbb{C}^N$ with sparsity S (i.e., the number of non-zero elements in $\mathbf{x}$) with $S \ll N$ can be recovered from the measurement $\mathbf{y} \in \mathbb{C}^K$, where $K \geq S \cdot \log N$, by finding the solution to the following optimization problem: minimize the ℓ_1 norm $\|\mathbf{x}\|_{\ell_1}$ subject to $\mathbf{y} = \mathbf{\Phi} \mathbf{x}$, where $\mathbf{\Phi}$ is the $K \times N$ *sensing matrix* (also called *measurement matrix*). Random sampling locations are selected offline from the field. We reconstruct the field using $S \ll N$ minimization technique of RCS. In our earlier work [12] we used a conventional lawn-mower trajectory to get a preliminary estimate of the field. In conventional lawnmower trajectory the field is sampled at locations equidistant from each other. The drawback of this approach is that if the width of the phenomenon is smaller than the distance between adjacent sampling locations taken by the lawnmower trajectory then the phenomenon will be not detected while reconstructing the field.

Traveling Salesman Problem (TSP): To collect field values using multiple vehicles from locations given by RCS technique we use multiple traveling salesman problem (mTSP) algorithms [13]. The mTSP consists of finding trajectories for all AUVs, who all start and end at the same location, such that each intermediate sampling location is visited exactly once and the total cost of visiting all nodes is minimized. The cost metric in our solution is time, i.e, we want all vehicles to finish at exactly the same time. Once measurements from all sampling locations have been obtained we use RCS technique to reconstruct the field.

Phase II: Once the preliminary estimate of the field is obtained in Phase I, we adaptively sample the field in Phase II. Phase II is divided into multiple micro-rounds. In each micro-round we aim to reconstruct the scalar field by minimizing an objective function. The objective function is to sample the field by minimizing the energy consumed to take samples while keeping the reconstruction
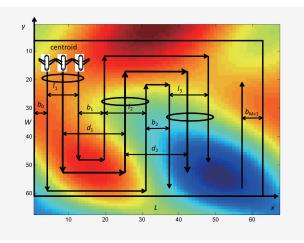
Figure 2: Trajectory planning for multiple vehicles for one micro-round (here $V = 3$).

error below a threshold value. The objective function is applied on the field at regular intervals. Each application of this objective function forms a micro-round and allows us to track the temporal variations in the field of interest. The micro-rounds are repeated until the field changes beyond a specified value in comparison to the field estimated in Phase 1, at this time Phase 1 is triggered again.

Optimal sampling strategy for a micro-round: To illustrate the idea of each micro-round in our solution, we start from the case when the number of vehicles is one, i.e, $V = 1$, The AUV will follow the lawn-mower trajectory to scan the region. At each micro-round of the scan, the AUV uses the field information it got from the previous micro-round to optimize its conventional lawn-mower trajectory. In other words, the AUV uses the field reconstructed during the $(r-1)^{th}$ micro-round to optimize its trajectory at the rth micro-round (shown in Fig. 1(c)), i.e., by calculating the optimal number M^* of segments and the distances d_m's ($m = 1, \ldots, M^*$) between two neighboring line segments. Based on the previous sampling information, the vehicle decides the optimal number M^* of segments that are parallel to the y-axis and the distances d_m's between consecutive segments, and then follows this optimal trajectory to take samples. Generally speaking, the reconstructed $\hat{f}$ has large error in regions with frequent changes as the reconstruction is less accurate. Therefore, d_m in these regions should be small. On the other hand, the reconstructed $\hat{f}$ has small error in regions with less changes, resulting in large d_m in these regions.

We now formulate an optimization problem for a micro-round where the maximal reconstruction energy should be minimized with the reconstruction error as a constraint. Based on the previous sampling information, the vehicle decides the optimal number M^* of segments that are parallel to the y-axis and the distances d_m's between consecutive segments, and then follows this optimal trajectory to take samples. We assume that multiple AUVs ($V > 1$) are used to sample the field. As $V > 1$, besides M^* and the distances d_m's between two neighboring line segments, we need to include the dimension of the whole team, as shown in Fig. 2. Suppose the AUVs form a linear formation of width l_m with the same distance between each pair of neighbors when they are taking samples at the mth segment. We denote the margin distances of the starting and ending segments by b_0 and b_{M+1}, respectively. Similarly to the case of a single vehicle, we should optimize M, d_m's, and l_m's ($m = 1, \ldots, M$).

Multi-Vehicle Energy Minimization Problem:

Find: $M^*, d_m^*, l_m^*; m = 1, \ldots, M^*$

Min: $E(S, M, \nu) = \sum_{v=1}^{V} E_{seg,v}(S, \nu) + E_{turn,v}(\theta_m) +$
$$+ N_{smp,v} E_{smp,v}$$

S.t.: $\dfrac{\sum_{x,y,z=1 \ldots X,Y,Z} |\hat{f}_r(x, y, z) - \hat{f}_{r-1}(x, y, z)|}{X \cdot Y \cdot Z} \leq \epsilon;$ (1)

$\alpha \cdot x + \beta \cdot y + \gamma \cdot z + \delta = 0.$ (2)

In this formulation, $\hat{f}_r(x, y, z)$ denotes the reconstructed field value at position (x, y, z) for the rth micro-round, l_m denotes the group width of these V AUVs, and X, Y, and Z represent the maximum values along each axis. Here, (2) represents a plane and for an horizontal plane $\alpha = \beta = 0$ and $\gamma = -1$ so that the equation of the plane becomes $z = \delta$. Also, $Z = 1$ for images of horizontal planes. Here, $E_v(S, M, \nu)$ represent an energy model, where $E_{seg,v}(S, \nu)$, $E_{turn,v}(\theta_m)$, and $E_{smp,v}$ represents the energy consumed while the vehicle travels through the line segments, makes turns, and takes one sample, respectively. $N_{smp,v}$ represents the total number of samples collected from vehicle v. Besides the energy consumption, the AUVs are constrained by the time constraint to finish one micro-round and by the dimension of the sampling field.

Reconstruction technique for a micro-round: As the objective function in our optimization is non-linear and depends on M, d_i's and l_i's, these two problems are in general non-linear optimization problems. To solve these two problems, we need to find $2M^* + 1$ optimal values (i.e., M^*, d_i, l_i, $i = 1, \ldots, M^*$). To solve both problems, the vehicles can send the samples they took to one vehicle that is called the *team leader*. This leader then estimates the field of interest $\hat{f}(x, y, z)$ using methods such as interpolation/extrapolation. We can estimate the range of M being $M \leq \min(L/d_{th}, T_{th} \cdot \nu/W)$. To solve it, we can do the exhaustive search after discretization. That is d_i and l_i can only take one value in the set $\{i \cdot L/N_L, i = 0, \ldots, N_L\}$ of N_L numbers. The computation complexity for the exhaustive search algorithm is $\mathcal{O}(M_{\min} \cdot N_L^{M_{\min}})$, where $M_{\min} = \min(L/d_{th}, T_{th} \cdot \nu/W)$. Further improvement to the exhaustive search algorithm can be to observe the characteristics of the field $\hat{f}(x, y, z)$. We also present results by interpolation using Radial Basis Function (RBF) [14]. RBF have been applied successfully to various application in environmental field and geostatistics [15, 16]. The reconstructed field using radial basis function is given as,

$$S(p) = \sum_{v=1}^{V} \sum_{i=1}^{I_v} \alpha_{v,i} \cdot \phi(p - p_{v,i}). \quad (3)$$

Here, $\phi(p)$ indicates a family of radial basis function, $p_{v,i}$ indicates the ith sample selected by the vth AUV (where I_v is the total number of samples selected by the vth AUV and the total number of AUVs is V). One basis function is centered at each sampled location. We first estimate the weights $\alpha_{v,i}$ from our known sampled locations using least square minimization and then and then use them to to estimate the field at all unknown locations by interpolation of measured data.

As mentioned earlier, Phase I of a new round is triggered when the reconstructed map (of the field of interest) of a micro-round differs significantly (by a pre-specified threshold) from the reconstructed map of its corresponding Phase I. However, Phase I of subsequent rounds need not be as comprehensive as that of the first round. Data from the last few micro-rounds of the recently con-
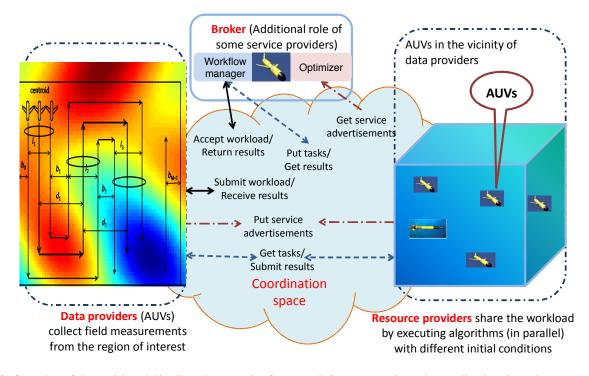
Figure 3: Overview of the envisioned distributed computing framework for compute-intensive applications in underwater networks.

cluded Phase II can be utilized smartly to improve the energy efficiency of Phase I (random compressive sensing) in the new round. This improvement exploits the fact that the field does not vary significantly over the span of a few micro-rounds, especially, if they are spaced less than a day apart.

Random compressive sensing, which is employed during Phase I typically employs one out of a number ideal sensing matrices all of which along with a particular sparse basis satisfy the incoherence requirement for sampling. One such sensing matrix can be superimposed on a matrix of spatially distributed measurements from the last few micro-rounds of a recently concluded Phase II to identify "empty" regions in space from where samples are missing. We can estimate the energy requirement of AUVs to collect random samples only from these empty regions. If this energy requirement is less than that of what is required for collection of random samples from the entire field for reconstruction, then data is collected only from the empty regions for the new Phase I resulting in further energy savings.

3.2 A Distributed Computing Framework for Multi-Vehicle Sampling

After the sampling of a region is complete the AUVs in the team send their data data to the leader AUV for global reconstruction. Also, the computational complexity of the optimization problem to detect samples is try high. To facilitate of aggregation of exchange of data between AUVs and support the compute intensive tasks we propose a distributed computing framework. To reduce the complexity of the above optimization for the leader, the computation can be distributed to the whole team of AUVs. To distribute the computation load to vehicles in the team, we envision that the computing and storage capabilities of the AUVs in the vicinity can be utilized to form an *elastic resource pool* that can process massive amounts of locally generated data in parallel. We propose a ubiquitous computing solution that is aimed at organizing AUVs in

the vicinity into a *wirelessly connected local distributed computing grid*. The collective computational capability of this distributed grid can be exploited to perform distributed computation. Figure 3 presents our distributed computing framework. In our distributed computing grid the leader is called *broker* and other AUVs are the service providers.

We propose a *resource provisioning framework* for distributed grids that runs at the broker. The framework facilitates interactions between data providers, which place service requests, and service providers, which dedicate a portion of their computational (CPU cycles), storage (volatile and non-volatile memory), and communication resources (i.e., network interface capacity) for servicing those requests. Our proposed resource provisioning framework strives to minimize the computational load on individual service providers by exploiting parallelism while incurring the minimal communication cost. The framework applies to applications exhibiting *data parallelism* (in which data is distributed across different parallel computing nodes that perform the same task) as well as to applications exhibiting *task parallelism* (in which parallel computing nodes may perform different tasks on the same or different data). Additionally, it can also facilitate storage of the collected samples and processed online information so to provide data and information whenever required for adaptive algorithms.

The broker shares the different tasks of the workload submitted by the data providers among the available service providers based on one of several possible policies. An example policy may be minimization of response time with emphasis on the proximity of data and computation while ensuring that none of the service providers is unfairly overloaded. Another policy might just place emphasis on response time without considering fairness. While the underutilized vehicles can be configured or setup to be service providers by default, adaptive mechanisms have to be formulated to incentivize AUVs that are part of the network to play the role of service providers.

Using this distributed computing framework, we can distribute the computation load among the AUVs in the team. To do this, we can decompose the centralized optimization problems in Sect. 3.1 into sub-problems that can be run in different AUVs. We can discretize the x direction into H_x values, which is then further partitioned into V intervals. These intervals are then distributed to the V vehicles of the team and each vehicle will estimate the team trajectory in its assigned interval. In this way the problem can be decomposed into sub-optimization problems for individual vehicles to solve. Note that the boundaries of these sub-problems should be the same for consecutive regions. That is, the ending point of one region should be the same as the starting point of the next region. In more detail, each vehicle solves for the same optimization as in Sect. 3.1 for their assigned sub-region. In addition, we add two more constraints for the starting and ending point of the planned trajectory - the starting point the trajectory in the one sub-region should be the same as the ending point in its previous sub-region and the ending point should be the same as the starting point in its next sub-region. These two constraints introduce coupling between consecutive sub-problems. Such coupling can be removed by adding an interface variable representing the constrained position between two consecutive sub-problems. In this way, the original centralized optimization problem can be decomposed into V sub-problems, which are then assigned to the individual vehicles. After the assigned sub-problem is solved, each vehicle sends the optimal parameters and trajectory back to the team leader so that the trajectory for the whole region is obtained.

We now discuss the communication aspect to facilitate the collection of samples by AUVs for reconstruction of the field. Before beginning the sampling mission the AUVs know the sampling locations in the field based on the field reconstructed in the previous micro-round. As a result each AUV can check itself its deviation from trajectory periodically. The only communication is at the end of each micro-round, where each AUVs communicates its sampling locations and the field values therein to the leader AUV. The leader performs a localized reconstruction.

3.3 Reliable Inter-AUV Communication

Next we explain our communication algorithm that select the best neighbor vehicle, the best number of samples and related information (which includes the sample value, the location, and time), and the optimal transmission power so that the end-to-end packet error rate can be maximized. The number of hops can be estimated by projecting the current distance to the neighbor to the distance to the team leader. Assume the current vehicle is v, we can formulate the following optimization problem for sample collection.

End-to-end PER Minimization Problem:

Find: $j* \in \mathcal{N}_v, P_{vj}^* \in [P_{\min}, P_{\max}],$
$$K_{smp}^* \in \{1, \ldots, K_{\max}\}$$

Min: $[PER(j, P_{vj}, K_{smp})]^{N_{hop}(j, dest)}$

S.t.:

$$PER(j, P_{vj}, K_{smp}) = 1 - (1 - BER(j, P_{vj}))^{L(K_{smp})}; \quad (4)$$

$$L(K_{smp}) = L_h + K_{smp} \cdot L_{smp}; \quad (5)$$

$$BER(j, P_{vj}) = g(SINR(j, P_{vj})); \quad (6)$$

$$SINR(j, P_{vj}) = \frac{P_{vj} \cdot (TL(d_{vj}))^{-1}}{\sum_{k \neq v} P_{kj} \cdot (TL(d_{kj}))^{-1} + N_0}; \quad (7)$$
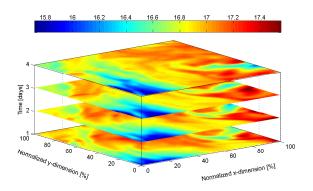
$$N_{hop}(v, j, dest) = \frac{d_{v, dest}}{projd_{vj}}. \quad (8)$$

Figure 4: Variation of a temperature [$^{\circ}$C] field over multiple days (Courtesy: http://ourocean.jpl.nasa.gov/).

Here $\mathcal{N}_v$ is the set of v's neighbor, P_{vj} is the transmission power from v to j, K_{smp} is the number of samples to put in this packet, $PER(j, P_{vj}, K_{smp})$ is the corresponding packet error rate from v to j, $BER(j, P_{vj})$ is the bit error rate, $L(K_{smp}$ is the length of packet in bits with L_h and L_{smp} being the packet header length and the length for one sample respectively. $BER(j, P_{vj})$ is generally estimated from SINR using function $g(SINR(j, P_{vj}))$ and $TL(d_{vj})$ is the transmission loss over the distance d_{vj} from v to j. Last, the number of hops to the destination $dest$ is estimated by dividing $d_{v, dest}$ - the distance from v to $dest$ - by the projected distance of d_{vj} to $d_{v, dest}$. By solving this question, we can find the optimal neighbor vehicle, transmission power, and the number of samples to transmit so that the end-to-end PER is minimized. The framework can enable the movement of the data between AUVs to aggregate the data at the leader and support global reconstruction of the field.

4. PERFORMANCE EVALUATION

We implemented and simulated our solution, and compared it against existing solutions such as the conventional lawn-mower-style sampling, DCS, and RCS. The lawn-mower sampling solution is based on the AUV-coordination solution proposed in [3]; the AUVs follow a lawn-mower trajectory and take measurements equidistant from each other. The RCS solution is based on [10] where measurements are taken at random locations in the field. For DCS the sampling locations are chosen using discrete chirp codes [17]. For both RCS and DCS, once the locations have been determined offline, a shortest-path algorithm is applied to calculate the trajectory of AUVs.

In our simulations, the temperature field to be sampled is a unit 2D square (i.e., 1×1 km^2) region on the ocean surface. Each AUV is assumed to move at a horizontal speed of 0.001 unit distance per second (e.g., 1 m/s in a 1×1 km^2 region). We assume that the user needs a temperature map of the 1 km^2 region (reconstructed using the data sampled by the AUVs) every *day*. We use Gaussian RBF for reconstruction of field from measurements. Performance of the aforementioned sampling strategies are analyzed in 2-day windows. This is because a 2-day window represents the worst-case scenario of our solution where Phase I is followed only by one micro-round in Phase II. However, based on our analysis of real data traces from [18], ocean surface temperature and salinity fields remain relatively stable over multiple days ($\sim$10) allowing for multiple micro-rounds in Phase II. For fair comparison, the other sampling techniques (RCS, DCS, and lawn-mower-style) are
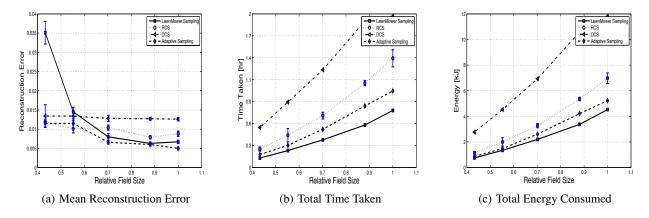
(a) Mean Reconstruction Error (b) Total Time Taken (c) Total Energy Consumed

Figure 5: Performance comparison of our adaptive sampling solution with existing solutions (averaged over multiple 2-day windows).

(a) Original Image (b) Lawn-mower-style horizontal sampling (c) Adaptive horizontal sampling

(d) Random Compressive Sensing (RCS) (e) Lawn-mower-style vertical sampling (f) Adaptive vertical sampling
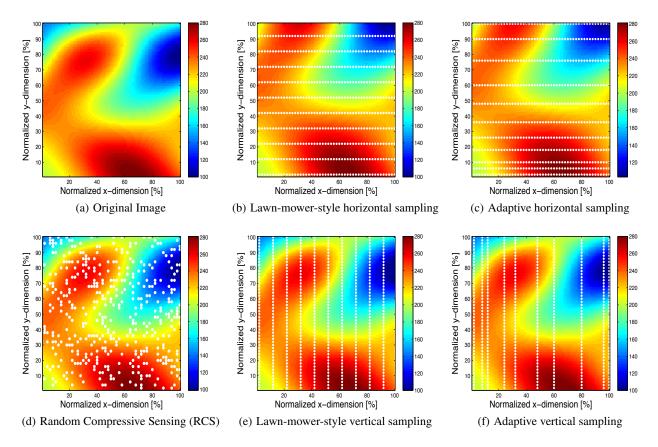
Figure 6: Illustration of the effect of angle of sampling (vertical or horizontal) on reconstruction accuracy and the motivation for Phase I (RCS) re-trigger.

repeated on both days to obtain the temperature map. In Fig. 4 the variation of temperature of a region with time is shown. The metrics used for comparison of our solution with existing solutions are: i) *mean reconstruction error* over two days (Fig. 5(a)), ii) *sum of time taken* by vehicles to sample the entire field over two days (Fig. 5(b)), and iii) *sum of energy consumed* by the AUVs over two days (Fig. 5(c)). The results presented are averaged over multiple 2-day windows for statistical relevance (95% confidence interval).

In Fig. 5(a), we see that the mean reconstruction error of our

solution is comparable to that of RCS and lower than the other sampling techniques even though we spend less time and energy compared to the other techniques as shown in Figs. 5(b) and 5(c), respectively. The main reason for this is that our solution factors the characteristics (in the spatial distribution) of the field of interest in the determination of sampling locations in the micro-rounds of Phase II as opposed to the other techniques, which repeat the same strategy on each of the three days. In other words, the competing approaches select fixed number of samples irrespective of the un-

derlying data, hence, are not adaptive to field measurements unlike our solution. The DCS solution using chirp codes requires that the sparsity of data to be much higher than that present in the temperature images considered in our simulations as a result of which the reconstruction error is very high.

We now present the motivation for re-triggering Phase I over time using an illustrative example. In Figs. 6(b) and 6(e), we present an example of a reconstructed field using lawn-mower-style horizontal and vertical sampling, respectively. Similarly, in Figs. 6(c) and 6(f), we present an example of a reconstructed field using adaptive horizontal and vertical sampling, respectively. Here, the sampling locations in the field are denoted by white dots. In lawn-mower-style sampling, the trajectories are equally spaced while in adaptive sampling the trajectory is chosen adaptively by our optimization algorithm, which takes the knowledge of spatial distribution of temperature into account. From the aforementioned set of figures it is clear that the angle of sampling (vertical or horizontal) has a significant impact on the reconstruction accuracy of the field of interest as shown in Fig. 6(a). This serves as the our primary motivation for re-triggering Phase I, which employs RCS, as the random sampling in RCS (shown in Fig. 6(d)) eliminates the effect of angle of sampling. Due to space limitations only a representative set of simulation results have been presented here. Comparison of different sampling strategies for reconstructing ocean salinity maps are available in a detailed technical report [19]. Also, insights on the typical number of micro-rounds in Phase II of our solution on real data traces as well as gains (in terms of time and energy) over other techniques are presented in [19].

5. CONCLUSION

We proposed a novel distributed adaptive sampling solution that can minimize the cost of sampling (in terms of time or energy expenditure) a 3D aquatic volume of interest using a team of autonomous underwater vehicles along with underwater acoustic communication protocols, which facilitate reliable inter-vehicle coordination. Our proposed solution not only captures the spatial distribution of the field of interest but also tracks the temporal variation of the same. Our communication solution enables timely and reliable reconstruction of the field by optimizing communication parameters at various protocol layers and by minimizing the end-to-end packet error rate. We have demonstrated the superiority of our proposed solution over the state of the art in terms of reconstruction accuracy and energy expenditure through extensive trace-driven simulations.

6. ACKNOWLEDGEMENTS

7. REFERENCES

[1] P. Lynch, "The origins of computer weather prediction and climate modeling," *Journal of Computational Physics (Elsevier)*, vol. 227, no. 7, pp. 3431–3444, Febuary 2008.

[2] T. N. Palmer, "Predicting uncertainty in forecasts of weather and climate," *European Centre for Medium-Range Weather Forecasts (ECMWF) Technical Memorandum*, vol. 294, November 1999.

[3] B. Chen and D. Pompili, "Team Formation and Steering Algorithms for Underwater Gliders using Acoustic Communication," *Computer Communications (Elsevier)*, vol. 35, no. 9, pp. 1017–1028, May 2012.

[4] N. K. Yilmaz, C. Evangelinos, P. F. J. Lermusiaux, and N. M. Patrikalakis, "Path Planning of Autonomous Underwater Vehicles for Adaptive Sampling Using Mixed Integer Linear Programming," *IEEE Journal of Oceanic Engineering*, vol. 33, no. 4, pp. 522–537, October 2008.

[5] E. Fiorelli, P. Bhatta, and N. E. Leonard, "Adaptive sampling using feedback control of an autonomous underwater glider fleet," in *Proc. of International Symposium on Unmanned Untethered Submersible Technology (UUST)*, Durham, NH, August 2003.

[6] D. L. Donoho, "Compressed Sensing," *IEEE Transactions on Information Theory*, vol. 52, no. 4, pp. 1289–1306, April 2006.

[7] A. Munafo, E. Simetti, A. Turetta, A. Caiti, and G. Casalino, "Autonomous Underwater Vehicle Teams for Adaptive Ocean Sampling: A Data-driven Approach," *Ocean Dynamics*, vol. 61, no. 11, pp. 1981–1994, July 2011.

[8] A. Alvarez, A. Caffaz, A. Caiti, G. Casalino, L. Gualdesi, A. Turetta, and R. Viviani, "Folaga: A low-cost autonomous underwater vehicle combining glider and auv capabilities," *Ocean Engineering*, vol. 36, no. 1, pp. 24–38, September 2008.

[9] D. Popa, A. Sanderson, R. Komerska, S. Mupparapu, D. Blidberg, and S. Chappel, "Adaptive sampling algorithms for multiple autonomous underwater vehicles," in *Proc. of IEEE International Conference on Autonomous Underwater Vehicles*, Sebasco Estates, Maine, June 2004.

[10] R. Hummel, S. Poduri, F. Hover, U. Mitra, and G. Sukhatme, "Mission design for compressive sensing with mobile robots," in *Proc. of IEEE International Conference on Robotics and Automation (ICRA)*, Shanghai, China, May 2011.

[11] R. Baraniuk, "Compressive sensing," *IEEE Signal Processing Magazine*, vol. 24, no. 4, pp. 118–121, July 2007.

[12] B. Chen, P. Pandey, and D. Pompili, "An Adaptive Sampling Solution using Autonomous Underwater Vehicles," in *Proc. of IFAC Conference on Manoeuvring and Control of Marine Craft (MCMC)*, Italy, August 2012.

[13] T. Bektas, "The multiple traveling salesman problem: an overview of formulations and solution procedures," *Omega*, vol. 34, no. 3, pp. 209–219, June 2006.

[14] R. Schaback, "Multivariate interpolation and approximation by translates of a basis function," *Series In Approximations and Decompositions*, vol. 6, pp. 491–514, June 1995.

[15] R. Hardy, "multiquadric-biharmonic method. 20 years of discovery 1968-1988," *Computers & Mathematics with Applications*, vol. 19, no. 8, pp. 163–208, January 1990.

[16] R. Franke, "Scattered data interpolation: Tests of some methods." *Math. Comput.*, vol. 38, no. 157, pp. 181–200, January 1982.

[17] L. Applebaum, S. Howard, S. Searle, and R. Calderbank, "Chirp sensing codes: Deterministic compressed sensing measurements for fast recovery," *Applied and Computational Harmonic Analysis (Elsevier)*, vol. 26, no. 2, pp. 283–290, November 2009.

[18] JPL, "OurOcean Portal, California Institute of Technology," 2012, http://ourocean.jpl.nasa.gov./.

[19] P. Pandey and D. Pompili, "Distributed Adaptive Sampling Algorithm for Autonomous Underwater Vehicles," 2012, http://www.eden.rutgers.edu/~pp395/tech_report.pdf.